



Synthesis, spectroscopic and Hirshfeld surface analysis and fluorescence studies of (2*E*,2'*E*)-3,3'-(1,4-phenylene)bis[1-(4-hydroxyphenyl)prop-2-en-1-one] *N,N*-dimethylformamide disolvate

Huey Chong Kwong,^a Ai Jia Sim,^b C. S. Chidan Kumar,^{c*} Ching Kheng Quah,^b Suchada Chantrapromma,^d S. Naveen^e and Ismail Warad^{f*}

Received 4 May 2018

Accepted 16 May 2018

Edited by D.-J. Xu, Zhejiang University (Yuquan Campus), China

Keywords: bischalcone; spectroscopy; centrosymmetric; Hirshfeld surface; fluorescence; crystal structure.

CCDC reference: 1449629

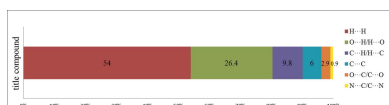
Supporting information: this article has supporting information at journals.iucr.org/e

^aSchool of Chemical Sciences, Universiti Sains Malaysia, Penang 11800 USM, Malaysia, ^bX-ray Crystallography Unit, School of Physics, Universiti Sains Malaysia, 11800 USM, Penang, Malaysia, ^cDepartment of Engineering Chemistry, Vidya Vikas Institute of Engineering & Technology, Visvesvaraya Technological University, Alanahally, Mysuru 570028, Karnataka, India, ^dDepartment of Chemistry, Faculty of Science, Prince of Songkla University, Hat-Yai, Songkhla 90112, Thailand, ^eDepartment of Physics, School of Engineering and Technology, Jain University, Bangalore 562 112, India, and ^fDepartment of Chemistry, Science College, An-Najah National University, PO Box 7, Nablus, West Bank, Palestinian Territories. *Correspondence e-mail: chidankumar@gmail.com, khalil.i@najah.edu

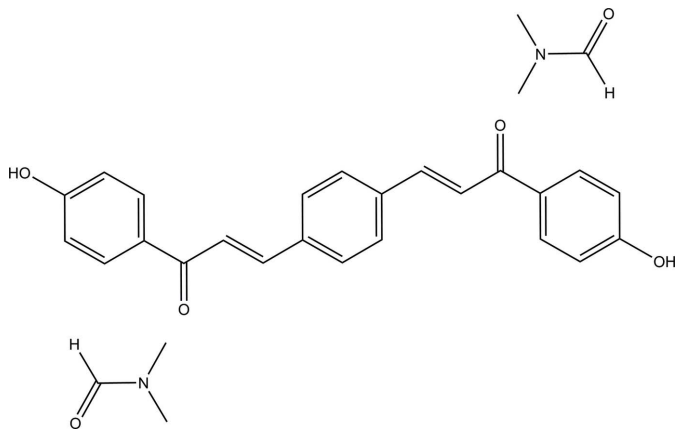
In the bischalcone molecule of the title compound, C₂₄H₁₈O₄·2C₃H₇NO, the central benzene and terminal hydroxyphenyl rings form a dihedral angle of 14.28 (11)° and the central C=C double bond adopts a *trans* configuration. In the crystal, the bischalcone and solvate molecules are interconnected *via* O—H···O hydrogen bonds, which were investigated by Hirshfeld surface analysis. Solid-state fluorescence was measured at λ_{ex} = 4400 Å. The emission wavelength appeared at 5510 Å, which corresponds to yellow light and the solid-state fluorescence quantum yield (F_f) is 0.18.

1. Chemical context

The development of new fluorescent probes has attracted much attention because of their applications in a wide range of electronic and optoelectronic devices related to telecommunications, optical computing, optical storage and optical information processing. Fluorescence generally occurs when a fluorescent probe (fluorophore) resonantly absorbs electromagnetic radiation that promotes it to an excited electronic state; subsequent relaxation of the excited state results in the emission of light, in which a portion of the excitation energy is lost through heat or vibration, and the rest is emitted at longer wavelengths compared to the excitation radiation. For a given fluorophore, the fluorescence intensity is directly proportional to the intensity of the radiation received. Fluorophores can be identified and quantified on the basis of their excitation and emission properties. Different materials may exhibit different colours and intensities of fluorescence despite seeming identical when observed in daylight conditions. In recent years, chalcones have been used in the field of material science as non-linear optical devices (Raghavendra *et al.*, 2017; Chandra Shekhara Shetty *et al.*, 2017), photorefractive polymers (Sun *et al.*, 1999), optical limiting (Shettigar *et al.*, 2006a; Chandra Shekhara Shetty *et al.*, 2016) and electrochemical sensing agents (Delavaux-Nicot *et al.*, 2007). The α,β-unsaturated ketone (C=C—C=O) moiety in the chalcone skeleton plays a vital role in its biological activities (Kumar *et al.*, 2013a,b). Apart from these biological activities,



the photophysical properties of chalcone derivatives have also attracted considerable attention from both chemists and physicists. In view of the above and as a part of our ongoing work on such molecules (Shettigar *et al.*, 2006b; Tejkiran *et al.*, 2016; Pramodh *et al.*, 2018; Naveen *et al.*, 2017), we herein report the synthesis, structure determination, Hirshfeld surface analysis and fluorescence properties of (2*E*,2'*E*)-3,3'-(1,4-phenylene)bis[1-(4-hydroxyphenyl)prop-2-en-1-one] *N,N*-dimethylformamide disolvate.



2. Structural commentary

The asymmetric unit of the title compound comprises of half of the bischalcone molecule, completed by inversion (symmetry operation $1 - x, 2 - y, -z$) and a DMF molecule (Fig. 1). The title compound crystallizes in the triclinic system with $Z = 1$ in space group $P\bar{1}$. The bischalcone molecule is constructed from two individually planar rings (central benzene and terminal hydroxyphenyl rings) and a C=C—C(=O)—C enone bridge with the central C=C double bond in a *trans* configuration. The hydroxyphenyl (C1—C6) and benzene (C10—C12/C10A—C12A) rings are almost parallel to each other, subtending a dihedral angle of $14.28(11)^\circ$. The enone fragment and its attached benzene ring are slightly twisted, as indicated by the torsion angles $O1—C7—C8—C9 = -5.6(4)^\circ$ and $C1—C6—C7—O1 = 1.7(4)^\circ$. All bond lengths and angles of the titled compound are in normal ranges (Allen *et al.*, 2002).

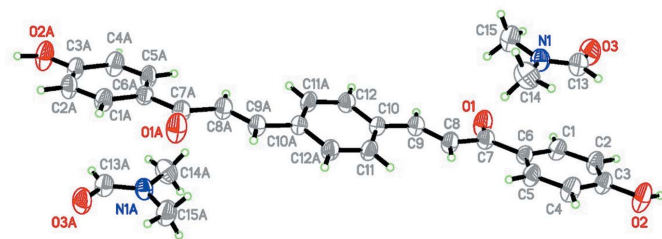


Figure 1
The molecular structure of the title compound, showing the atom-labelling scheme, with 40% probability displacement ellipsoids. Atoms labelled with the suffix A are generated by the symmetry operation $1 - x, 2 - y, -z$.

Table 1
Hydrogen-bond geometry ($\text{\AA}, ^\circ$).

$D-H \cdots A$	$D-H$	$H \cdots A$	$D \cdots A$	$D-H \cdots A$
$O2-H2B \cdots O3^i$	0.99 (4)	1.63 (5)	2.592 (3)	162 (4)

Symmetry code: (i) $-x, -y, -z + 1$.

3. Supramolecular features

In the crystal, the components are linked by $O2-H2B \cdots O3^i$ hydrogen bonds, which connect the DMF solvate molecules to both terminal 4-hydroxyphenyl rings of the main molecules (Fig. 2, Table 1).

4. Database survey

A search of the Cambridge Structural Database (CSD, Version 5.39, last update November 2016; Groom *et al.*, 2016) using (2*E*,2'*E*)-3,3'-(1,4-phenylene)bis(1-phenylprop-2-en-1-one) as main skeleton revealed the presence of four structures containing a similar bis-chalcone moiety to the title compound but with different substituents on the terminal phenyl rings, *viz.* 3,3'-(1,4-phenylene)bis[1-(*X*)prop-2-en-1-one], where *X* = 2-hydroxyphenyl (Gaur & Mishra, 2013), 4-chlorophenyl (KIKFUG; Harrison *et al.*, 2007), 4-methoxyphenyl (Harrison *et al.*, 2007a) and 3,4-methoxyphenyl (Harrison *et al.*, 2007b). In these four compounds, the dihedral angles between the central and terminal phenyl ring are in the range 10.91 – 46.27° . In the positional isomer of the title compound, the 2-hydroxyphenyl moiety forms a dihedral angle of 10.91° with the benzene ring, compared to $14.28(11)^\circ$ in the title compound. The difference may arise from the intramolecular hydrogen bond between 2-hydroxyphenyl unit and the adjacent carbonyl moiety.

5. Hirshfeld surface analysis

Hirshfeld surface analysis (McKinnon *et al.*, 2004, 2007; Spackman & Jayatilaka, 2009; Spackman & McKinnon, 2002) was undertaken to quantify and give visual confirmation of the intermolecular interaction, and to explain the observed crystal structure. The d_{norm} surface plots, electrostatic potential and 2D fingerprint plots were generated by *CrystalExplorer 3.1*

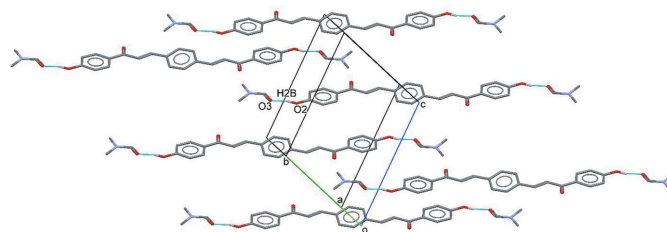


Figure 2
Partial crystal packing, showing the $O-H \cdots O$ hydrogen bonds (Table 1) between the bischalcone and DMF solvate molecules.

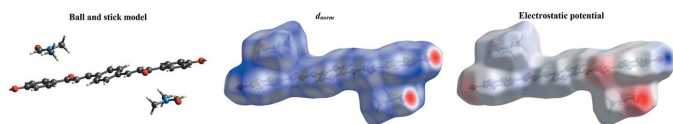


Figure 3
 d_{norm} and electrostatic potential mapped on Hirshfeld surfaces to visualize the intermolecular contacts in the title compound. The molecule in the ball-and-stick model is in the same orientation as for the Hirshfeld surface and electrostatic potential plots.

(Wolff *et al.*, 2012). The red spots on the d_{norm} surface arise as a result of the short interatomic contact; the positive electrostatic potential (blue regions) over the surface indicate hydrogen-donor potential, whereas the hydrogen-bond acceptors are represented by negative electrostatic potential (red regions). The d_{norm} surface plots and electrostatic potential of the title compound are shown in Fig. 3.

The surface shows a red spot on the hydroxyl and carbonyl groups of the main molecule and solvate, respectively. This is a result of the $\text{O2} \cdots \text{H2B} \cdots \text{O3}$ hydrogen bonds present in the structure (Fig. 4*a*). These observations are further confirmed by the respective electrostatic potential map in which the atoms involved in the formation of hydrogen bonds are seen as blue (hydrogen-bond donor) and red (hydrogen-bond acceptor) spots (Fig. 4*b*). The corresponding fingerprint plots (FP) for Hirshfeld surfaces show characteristic pseudo-symmetry wings in the d_e and d_i diagonal axes in the overall 2D FP (Fig. 5*a*). $\text{H} \cdots \text{H}$ contacts (*i.e.* dispersive forces) make the greatest percentage contribution to the Hirshfeld surface, followed by $\text{O} \cdots \text{H}/\text{H} \cdots \text{O}$ and $\text{C} \cdots \text{H}/\text{H} \cdots \text{C}$ contacts (Fig. 6). The $\text{H} \cdots \text{H}$ contacts appear as the largest region on the fingerprint plot with a high concentration in the middle region, at $d_e = d_i \sim 1.2 \text{ \AA}$ with an overall contribution to the Hirshfeld surface of 54.0% (Fig. 5*b*). The reciprocal $\text{O} \cdots \text{H}/\text{H} \cdots \text{O}$ interaction (26.4%) appears as two sharp symmetric spikes in the FP plot, which is characteristic of a strong hydrogen-bonding interaction, at $d_e + d_i \simeq 1.7 \text{ \AA}$ (Fig. 5*c*). Two symmetrical broad blunted wings corresponding to the $\text{C} \cdots \text{H}/$

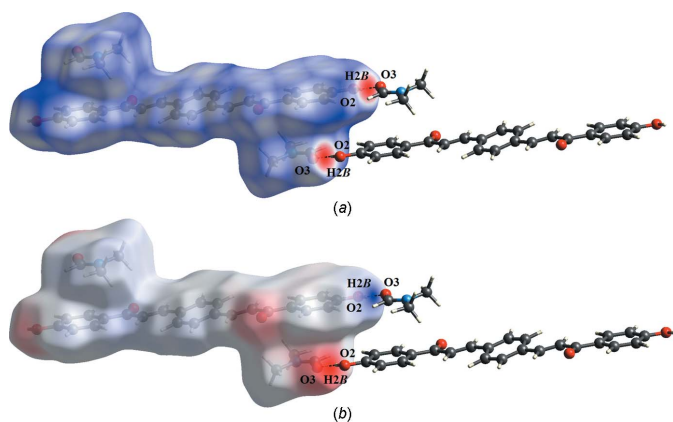


Figure 4
 (a) d_{norm} and (b) electrostatic potential mapped on Hirshfeld surfaces in order to visualize the intermolecular $\text{O} \cdots \text{H} \cdots \text{O}$ interactions in the title compound.

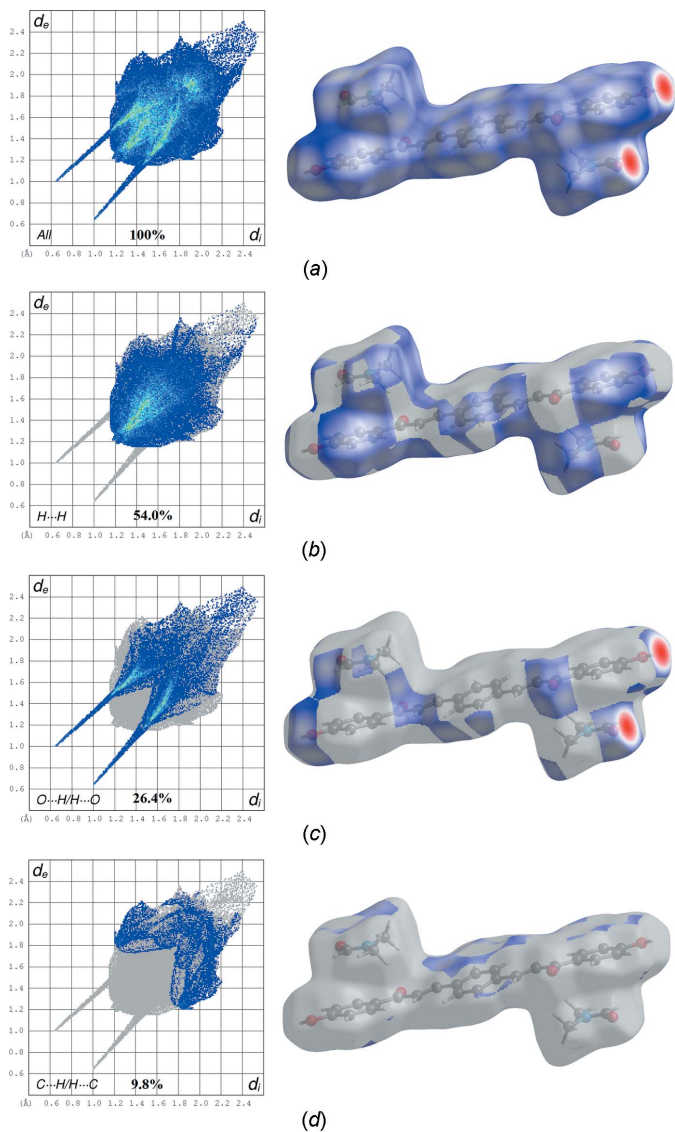


Figure 5
 The two-dimensional fingerprint plots for the title compound showing contributions from different contacts; the views on the right highlight the relevant surface patches associated with the specific contacts.

$\text{H} \cdots \text{C}$ interaction (with a 9.8% contribution) appear at $d_e + d_i \simeq 3.0 \text{ \AA}$ (Fig. 5*d*). Analysis of the close contact on the d_{norm} surface plot suggests that the $\text{C} \cdots \text{H}/\text{H} \cdots \text{C}$ interaction might arise from weak $\text{C} \cdots \text{H} \cdots \pi$ and $\text{C} \cdots \text{H} \cdots \text{alkene}$ interactions between the solvate and main molecules (Fig. 7).

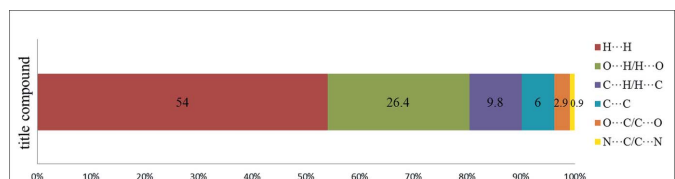


Figure 6
 Percentage contributions of the various intermolecular contacts contributing to the Hirshfeld surfaces of the title compound.

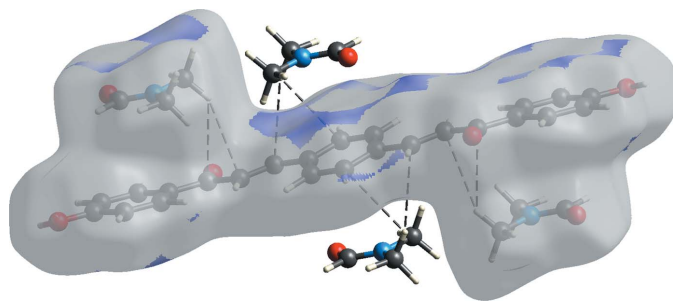


Figure 7
 d_{norm} mapped on Hirshfeld surfaces to visualize the weak intermolecular C–H... π and C–H...alkene interactions in the title compound.

6. Solid-state fluorescence studies

A powder sample of the subject compound (0.72 mol) was heaped in the tray, covered with a quartz plate and was then fixed in the fluorescence spectrometer. The solid-state fluorescence properties were measured at the excitation wavelength (λ_{ex}) of 4400 Å, which was selected from the absorption spectrum of the compound. The difference in the relative intensities of reflections between the sample and MgO powder was calibrated using diffusion reflections in a non-absorbed wavelength, in the present case this was 6500 Å. Finally, the fluorescence quantum yield (F_f) was determined by Wrighton's method and calculated according to the $\Phi_f = j_f / (\Upsilon j_o - j)$ (Wrighton *et al.*, 1974) where, j_f is the fluorescence intensity of the sample, Υ the calibration factor, j_o the back-scattered intensity of excitation light from a blank (here MgO) and j the back-scattered intensity of a loaded sample. The solid-state excitation and emission spectrum of the title compound (λ_{ex} at 4400 Å) is shown in Fig. 8. The emission wavelength (blue line) appears at 5510 Å, which corresponds to yellow light. The solid-state fluorescence quantum yield (F_f) of the title compound is 0.18.

7. Synthesis and crystallization

A mixture of corresponding 4-hydroxyacetophenone (0.02 mol) and terephthalaldehyde (0.01 mol) was dissolved

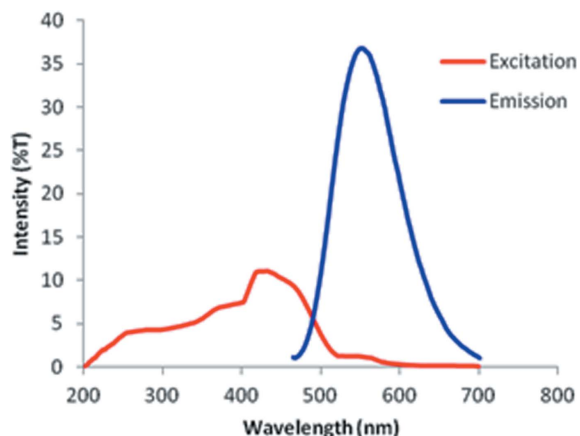


Figure 8
 Solid-state excitation and emission spectrum for the title compound

Table 2
 Experimental details.

Crystal data	
Chemical formula	$\text{C}_{24}\text{H}_{18}\text{O}_4 \cdot 2\text{C}_3\text{H}_7\text{NO}$
M_r	516.57
Crystal system, space group	Triclinic, $P\bar{1}$
Temperature (K)	294
a, b, c (Å)	6.0569 (5), 9.5801 (5), 11.9941 (8)
α, β, γ (°)	72.867 (2), 84.649 (2), 86.710 (2)
V (Å ³)	661.86 (8)
Z	1
Radiation type	Mo $K\alpha$
μ (mm ⁻¹)	0.09
Crystal size (mm)	0.25 × 0.24 × 0.10
Data collection	
Diffractometer	Bruker APEXII DUO CCD area-detector
Absorption correction	Multi-scan (<i>SADABS</i> ; Bruker, 2012)
$T_{\text{min}}, T_{\text{max}}$	0.961, 0.991
No. of measured, independent and observed [$I > 2\sigma(I)$] reflections	21963, 3039, 1944
R_{int}	0.043
$(\sin \theta/\lambda)_{\text{max}}$ (Å ⁻¹)	0.650
Refinement	
$R[F^2 > 2\sigma(F^2)], wR(F^2), S$	0.057, 0.177, 1.07
No. of reflections	3039
No. of parameters	178
H-atom treatment	H atoms treated by a mixture of independent and constrained refinement
$\Delta\rho_{\text{max}}, \Delta\rho_{\text{min}}$ (e Å ⁻³)	0.17, -0.19

Computer programs: *APEX2* and *SAINT* (Bruker, 2012), *SHELXS97* (Sheldrick, 2008), *SHELXL2013* (Sheldrick, 2015), *Mercury* (Macrae *et al.*, 2006) and *PLATON* (Spek, 2009).

in methanol (20 mL). A catalytic amount of NaOH was added to the solution dropwise with vigorous stirring. The reaction mixture was stirred for about 5–6 h at room temperature. The resultant crude product was filtered, washed successively with distilled water and recrystallized from acetone solution. Crystals suitable for X-ray diffraction studies were obtained by the slow evaporation technique using DMF as solvent. Yield: 85%, m.p. = 544–546 K.

FT-IR [ATR (solid) cm⁻¹]: 3193 (O–H, ν), 3193 (Ar, C–H, ν), 2945 (methyl, C–H, ν s), 2884 (methyl, C–H, ν), 1605 (C=O, ν), 1586, 1336 (Ar, C=C, ν), 1221 (C–O, ν), 1169 (C–N, ν). ¹H NMR (500 MHz, DMSO): δ (ppm) 8.120–8.103 (d , 4H, $J = 8.7$ Hz, ¹CH, ⁵CH), 8.028–7.997 (d , 2H, $J = 15.6$ Hz, ⁸CH), 7.964 (s , 4H, ¹¹CH, ¹²CH), 7.737–7.706 (d , 2H, $J = 15.6$ Hz, ⁹CH), 6.931–6.914 (d , 4H, $J = 8.7$ Hz, ²CH, ⁴CH); ¹³C NMR (125 MHz, DMSO): δ ppm 187.05 (C7), 162.29 (C3), 141.86 (C9), 136.65 (C10), 131.28 (C1, C5), 129.92 (C6), 129.19 (C11, C12), 123.05 (C8), 115.39 (C2, C4).

8. Refinement

Crystal data, data collection and structure refinement details are summarized in Table 2. The O-bound H atom was located in a difference-Fourier map and refined freely. C-bound H atoms were positioned geometrically [C–H = 0.93–0.96 Å]

and refined using a riding model with $U_{\text{iso}}(\text{H}) = 1.5U_{\text{eq}}(\text{C-methyl})$ and $1.2U_{\text{eq}}(\text{C})$ for other H atoms.

Acknowledgements

The authors extend their appreciation to the Vidya Vikas Research & Development Centre for the facilities and encouragement.

Funding information

HCK thanks the Malaysian Government for a MyBrain15 (MyPhD) scholarship. The authors thank the Malaysian Government and Universiti Sains Malaysia (USM) for the Research University Individual Grant (1001/PFIZIK/811278).

References

- Allen, F. H. (2002). *Acta Cryst.* **B58**, 380–388.
- Bruker (2012). *APEX2*, *SAINT* and *SADABS*. Bruker AXS Inc., Madison, Wisconsin, USA.
- Chandra Shekhara Shetty, T., Chidan Kumar, C. S., Gagan Patel, K. N., Chia, T. S., Dharmaparakash, S. M., Ramasami, P., Umar, Y., Chandrāju, S. & Quah, C. K. (2017). *J. Mol. Struct.* **1143**, 306–317.
- Chandra Shekhara Shetty, T., Raghavendra, S., Chidan Kumar, C. S. & Dharmaparakash, S. M. (2016). *Appl. Phys. B*, **122**, 205–.
- Delavaux-Nicot, B., Maynadié, J., Lavabre, D. & Fery-Forgues, S. (2007). *J. Organomet. Chem.* **692**, 874–886.
- Gaur, R. & Mishra, L. (2013). *RSC Adv.* **3**, 12210–12219.
- Groom, C. R., Bruno, I. J., Lightfoot, M. P. & Ward, S. C. (2016). *Acta Cryst.* **B72**, 171–179.
- Harrison, W. T. A., Ravindra, H. J., Kumar, M. R. S. & Dharmaparakash, S. M. (2007). *Acta Cryst.* **E63**, o3702.
- Harrison, W. T. A., Ravindra, H. J., Suresh Kumar, M. R. & Dharmaparakash, S. M. (2007a). *Acta Cryst.* **E63**, o3067.
- Harrison, W. T. A., Ravindra, H. J., Suresh Kumar, M. R. & Dharmaparakash, S. M. (2007b). *Acta Cryst.* **E63**, o3068.
- Kumar, C., Loh, W. S., Ooi, C., Quah, C. & Fun, H. K. (2013a). *Molecules*, **18**, 12707–12724.
- Kumar, C. S., Loh, W. S., Ooi, C. W., Quah, C. K. & Fun, H. K. (2013b). *Molecules*, **18**, 11996–12011.
- Macrae, C. F., Edgington, P. R., McCabe, P., Pidcock, E., Shields, G. P., Taylor, R., Towler, M. & van de Streek, J. (2006). *J. Appl. Cryst.* **39**, 453–457.
- McKinnon, J. J., Jayatilaka, D. & Spackman, M. A. (2007). *Chem. Commun.* 3814–3816.
- McKinnon, J. J., Spackman, M. A. & Mitchell, A. S. (2004). *Acta Cryst.* **B60**, 627–668.
- Naveen, S., Ming, L. S., Jamalis, J., Ananda Kumar, C. S. & Lokanath, N. K. (2017). *Chem. Data Coll.* **7**, 58–67.
- Pramodh, B., Lokanath, N. K., Naveen, S., Naresh, P., Ganguly, S. & Panda, J. (2018). *J. Mol. Struct.* **1161**, 9–17.
- Raghavendra, S., Chidan Kumar, C. S., Shetty, T. C. S., Lakshminarayana, B. N., Quah, C. K., Chandrāju, S., Ananthnag, G. S., Gonsalves, R. A. & Dharmaparakash, S. M. (2017). *Results Phys.* **7**, 2550–2556.
- Sheldrick, G. M. (2008). *Acta Cryst.* **A64**, 112–122.
- Sheldrick, G. M. (2015). *Acta Cryst.* **C71**, 3–8.
- Shettigar, S., Chandrasekharan, K., Umesh, G., Sarojini, B. K. & Narayana, B. (2006). *Polymer*, **47**, 3565–3567.
- Shettigar, V., Patil, P. S., Naveen, S., Dharmaparakash, S. M., Sridhar, M. A. & Shashidhara Prasad, J. (2006). *J. Cryst. Growth*, **295**, 44–49.
- Spackman, M. A. & Jayatilaka, D. (2009). *CrystEngComm*, **11**, 19–32.
- Spackman, M. A. & McKinnon, J. J. (2002). *CrystEngComm*, **4**, 378–392.
- Spek, A. L. (2009). *Acta Cryst.* **D65**, 148–155.
- Sun, S.-J., Schwarz, G., Kricheldorf, H. R. & Chang, T.-C. (1999). *J. Polym. Sci. A Polym. Chem.* **37**, 1125–1133.
- Tejkiran, P. J., Brahma Teja, M. S., Sai Siva Kumar, P., Sankar, P., Philip, R., Naveen, S., Lokanath, N. K. & Nageswara Rao, G. (2016). *J. Photochem. Photobiol. Chem.* **324**, 33–39.
- Wolff, S. K., Grimwood, D. J., McKinnon, J. J., Turner, M. J., Jayatilaka, D. & Spackman, M. A. (2012). *University of Western Australia*.
- Wrighton, M. S., Ginley, D. S. & Morse, D. L. (1974). *J. Phys. Chem.* **78**, 2229–2233.

supporting information

Acta Cryst. (2018). E74, 835-839 [https://doi.org/10.1107/S2056989018007429]

Synthesis, spectroscopic and Hirshfeld surface analysis and fluorescence studies of (2*E*,2'*E*)-3,3'-(1,4-phenylene)bis[1-(4-hydroxyphenyl)prop-2-en-1-one] *N,N*-dimethylformamide disolvate

Huey Chong Kwong, Ai Jia Sim, C. S. Chidan Kumar, Ching Kheng Quah, Suchada Chantrapromma, S. Naveen and Ismail Warad

Computing details

Data collection: *APEX2* (Bruker, 2012); cell refinement: *SAINT* (Bruker, 2012); data reduction: *SAINT* (Bruker, 2012); program(s) used to solve structure: *SHELXS97* (Sheldrick, 2008); program(s) used to refine structure: *SHELXL2013* (Sheldrick, 2015); molecular graphics: *SHELXL2013* (Sheldrick, 2015) and *Mercury* (Macrae *et al.*, 2006); software used to prepare material for publication: *SHELXL2013* (Sheldrick, 2015) and *PLATON* (Spek, 2009).

(2*E*,2'*E*)-3,3'-(1,4-phenylene)bis[1-(4-hydroxyphenyl)prop-2-en-1-one] *N,N*-dimethylformamide disolvate

Crystal data

$C_{24}H_{18}O_4 \cdot 2C_3H_7NO$
 $M_r = 516.57$
 Triclinic, $P\bar{1}$
 $a = 6.0569$ (5) Å
 $b = 9.5801$ (5) Å
 $c = 11.9941$ (8) Å
 $\alpha = 72.867$ (2)°
 $\beta = 84.649$ (2)°
 $\gamma = 86.710$ (2)°
 $V = 661.86$ (8) Å³

$Z = 1$
 $F(000) = 274$
 $D_x = 1.296$ Mg m⁻³
 Mo $K\alpha$ radiation, $\lambda = 0.71073$ Å
 Cell parameters from 4190 reflections
 $\theta = 2.4$ – 23.5 °
 $\mu = 0.09$ mm⁻¹
 $T = 294$ K
 Block, colourless
 $0.25 \times 0.24 \times 0.10$ mm

Data collection

Bruker APEXII DUO CCD area-detector diffractometer
 Radiation source: fine-focus sealed tube
 Graphite monochromator
 φ and ω scans
 Absorption correction: multi-scan (SADABS; Bruker, 2012)
 $T_{\min} = 0.961$, $T_{\max} = 0.991$

21963 measured reflections
 3039 independent reflections
 1944 reflections with $I > 2\sigma(I)$
 $R_{\text{int}} = 0.043$
 $\theta_{\max} = 27.5$ °, $\theta_{\min} = 1.8$ °
 $h = -7 \rightarrow 7$
 $k = -12 \rightarrow 12$
 $l = -15 \rightarrow 15$

Refinement

Refinement on F^2
 Least-squares matrix: full
 $R[F^2 > 2\sigma(F^2)] = 0.057$
 $wR(F^2) = 0.177$
 $S = 1.07$

3039 reflections
 178 parameters
 0 restraints
 Hydrogen site location: mixed

H atoms treated by a mixture of independent
and constrained refinement
 $w = 1/[\sigma^2(F_o^2) + (0.0694P)^2 + 0.2543P]$
where $P = (F_o^2 + 2F_c^2)/3$

$(\Delta/\sigma)_{\max} < 0.001$
 $\Delta\rho_{\max} = 0.17 \text{ e } \text{\AA}^{-3}$
 $\Delta\rho_{\min} = -0.19 \text{ e } \text{\AA}^{-3}$

Special details

Geometry. All esds (except the esd in the dihedral angle between two l.s. planes) are estimated using the full covariance matrix. The cell esds are taken into account individually in the estimation of esds in distances, angles and torsion angles; correlations between esds in cell parameters are only used when they are defined by crystal symmetry. An approximate (isotropic) treatment of cell esds is used for estimating esds involving l.s. planes.

Fractional atomic coordinates and isotropic or equivalent isotropic displacement parameters (\AA^2)

	<i>x</i>	<i>y</i>	<i>z</i>	$U_{\text{iso}}^*/U_{\text{eq}}$
O1	-0.1262 (3)	0.5766 (2)	0.23944 (17)	0.0750 (6)
O2	0.2445 (3)	0.0650 (2)	0.64822 (17)	0.0793 (6)
H2B	0.108 (7)	0.010 (5)	0.682 (4)	0.145 (15)*
C1	-0.0487 (4)	0.3283 (3)	0.4223 (2)	0.0545 (6)
H1A	-0.1859	0.3421	0.3911	0.065*
C2	-0.0096 (4)	0.2057 (3)	0.5127 (2)	0.0571 (6)
H2A	-0.1197	0.1376	0.5423	0.069*
C3	0.1943 (4)	0.1834 (3)	0.5599 (2)	0.0542 (6)
C4	0.3540 (4)	0.2863 (3)	0.5152 (2)	0.0643 (7)
H4A	0.4909	0.2727	0.5468	0.077*
C5	0.3131 (4)	0.4087 (3)	0.4244 (2)	0.0557 (6)
H5A	0.4233	0.4767	0.3951	0.067*
C6	0.1110 (3)	0.4324 (2)	0.37597 (18)	0.0460 (5)
C7	0.0568 (4)	0.5610 (2)	0.2773 (2)	0.0527 (6)
C8	0.2297 (4)	0.6688 (2)	0.2225 (2)	0.0552 (6)
H8A	0.3635	0.6600	0.2566	0.066*
C9	0.2000 (4)	0.7762 (2)	0.1276 (2)	0.0503 (5)
H9A	0.0634	0.7814	0.0968	0.060*
C10	0.3566 (3)	0.8892 (2)	0.06404 (18)	0.0452 (5)
C11	0.5544 (4)	0.9078 (2)	0.1063 (2)	0.0515 (6)
H11A	0.5925	0.8463	0.1781	0.062*
C12	0.3042 (4)	0.9840 (2)	-0.0435 (2)	0.0513 (6)
H12A	0.1716	0.9740	-0.0733	0.062*
N1	0.3441 (3)	0.2611 (2)	0.16532 (17)	0.0539 (5)
O3	0.0634 (3)	0.1066 (2)	0.23142 (17)	0.0752 (6)
C13	0.2500 (4)	0.1452 (3)	0.2375 (2)	0.0610 (6)
H13A	0.3312	0.0880	0.2977	0.073*
C14	0.5659 (4)	0.3002 (3)	0.1757 (3)	0.0788 (8)
H14A	0.6290	0.2276	0.2392	0.118*
H14B	0.5611	0.3935	0.1906	0.118*
H14C	0.6553	0.3055	0.1042	0.118*
C15	0.2266 (5)	0.3526 (3)	0.0692 (3)	0.0767 (8)
H15A	0.0810	0.3160	0.0728	0.115*
H15B	0.3065	0.3518	-0.0036	0.115*
H15C	0.2142	0.4508	0.0746	0.115*

Atomic displacement parameters (\AA^2)

	U^{11}	U^{22}	U^{33}	U^{12}	U^{13}	U^{23}
O1	0.0553 (10)	0.0705 (12)	0.0816 (13)	-0.0128 (9)	-0.0211 (9)	0.0120 (10)
O2	0.0605 (11)	0.0750 (13)	0.0769 (13)	-0.0169 (9)	-0.0191 (9)	0.0242 (10)
C1	0.0427 (12)	0.0581 (14)	0.0556 (13)	-0.0102 (10)	-0.0092 (10)	-0.0021 (11)
C2	0.0456 (12)	0.0556 (14)	0.0594 (14)	-0.0185 (10)	-0.0057 (10)	0.0034 (11)
C3	0.0496 (12)	0.0534 (13)	0.0500 (13)	-0.0106 (10)	-0.0049 (10)	0.0018 (10)
C4	0.0446 (12)	0.0718 (17)	0.0646 (15)	-0.0158 (11)	-0.0162 (11)	0.0047 (13)
C5	0.0469 (12)	0.0555 (14)	0.0556 (14)	-0.0185 (10)	-0.0063 (10)	0.0018 (11)
C6	0.0460 (11)	0.0456 (12)	0.0431 (11)	-0.0080 (9)	-0.0033 (9)	-0.0065 (9)
C7	0.0500 (13)	0.0511 (13)	0.0525 (13)	-0.0072 (10)	-0.0079 (10)	-0.0062 (10)
C8	0.0517 (13)	0.0524 (13)	0.0545 (14)	-0.0100 (10)	-0.0106 (10)	-0.0012 (11)
C9	0.0473 (12)	0.0462 (12)	0.0516 (13)	-0.0047 (9)	-0.0045 (9)	-0.0047 (10)
C10	0.0476 (11)	0.0393 (11)	0.0445 (12)	-0.0030 (9)	-0.0027 (9)	-0.0060 (9)
C11	0.0558 (13)	0.0463 (12)	0.0445 (12)	-0.0046 (10)	-0.0115 (10)	0.0018 (9)
C12	0.0496 (12)	0.0490 (13)	0.0511 (13)	-0.0069 (10)	-0.0127 (10)	-0.0047 (10)
N1	0.0451 (10)	0.0505 (11)	0.0621 (12)	-0.0071 (8)	-0.0028 (9)	-0.0097 (9)
O3	0.0622 (11)	0.0740 (12)	0.0797 (13)	-0.0249 (9)	0.0030 (9)	-0.0060 (10)
C13	0.0598 (15)	0.0552 (15)	0.0622 (15)	-0.0043 (12)	-0.0051 (11)	-0.0074 (12)
C14	0.0536 (15)	0.083 (2)	0.104 (2)	-0.0178 (14)	-0.0046 (14)	-0.0301 (17)
C15	0.0751 (18)	0.0691 (18)	0.0739 (19)	-0.0094 (14)	-0.0138 (14)	0.0016 (14)

Geometric parameters (\AA , $^\circ$)

O1—C7	1.221 (3)	C9—H9A	0.9300
O2—C3	1.347 (3)	C10—C11	1.383 (3)
O2—H2B	0.99 (4)	C10—C12	1.393 (3)
C1—C2	1.370 (3)	C11—C12 ⁱ	1.377 (3)
C1—C6	1.387 (3)	C11—H11A	0.9300
C1—H1A	0.9300	C12—C11 ⁱ	1.377 (3)
C2—C3	1.386 (3)	C12—H12A	0.9300
C2—H2A	0.9300	N1—C13	1.312 (3)
C3—C4	1.377 (3)	N1—C14	1.441 (3)
C4—C5	1.374 (3)	N1—C15	1.445 (3)
C4—H4A	0.9300	O3—C13	1.224 (3)
C5—C6	1.382 (3)	C13—H13A	0.9300
C5—H5A	0.9300	C14—H14A	0.9600
C6—C7	1.481 (3)	C14—H14B	0.9600
C7—C8	1.480 (3)	C14—H14C	0.9600
C8—C9	1.310 (3)	C15—H15A	0.9600
C8—H8A	0.9300	C15—H15B	0.9600
C9—C10	1.466 (3)	C15—H15C	0.9600
C3—O2—H2B	110 (2)	C11—C10—C12	117.98 (19)
C2—C1—C6	121.8 (2)	C11—C10—C9	123.14 (19)
C2—C1—H1A	119.1	C12—C10—C9	118.88 (19)
C6—C1—H1A	119.1	C12 ⁱ —C11—C10	121.0 (2)

C1—C2—C3	119.8 (2)	C12 ⁱ —C11—H11A	119.5
C1—C2—H2A	120.1	C10—C11—H11A	119.5
C3—C2—H2A	120.1	C11 ⁱ —C12—C10	121.0 (2)
O2—C3—C4	118.0 (2)	C11 ⁱ —C12—H12A	119.5
O2—C3—C2	123.0 (2)	C10—C12—H12A	119.5
C4—C3—C2	119.0 (2)	C13—N1—C14	122.5 (2)
C5—C4—C3	120.6 (2)	C13—N1—C15	119.9 (2)
C5—C4—H4A	119.7	C14—N1—C15	117.6 (2)
C3—C4—H4A	119.7	O3—C13—N1	124.9 (2)
C4—C5—C6	121.1 (2)	O3—C13—H13A	117.6
C4—C5—H5A	119.4	N1—C13—H13A	117.6
C6—C5—H5A	119.4	N1—C14—H14A	109.5
C5—C6—C1	117.6 (2)	N1—C14—H14B	109.5
C5—C6—C7	123.92 (19)	H14A—C14—H14B	109.5
C1—C6—C7	118.46 (19)	N1—C14—H14C	109.5
O1—C7—C8	120.2 (2)	H14A—C14—H14C	109.5
O1—C7—C6	120.7 (2)	H14B—C14—H14C	109.5
C8—C7—C6	119.10 (19)	N1—C15—H15A	109.5
C9—C8—C7	122.0 (2)	N1—C15—H15B	109.5
C9—C8—H8A	119.0	H15A—C15—H15B	109.5
C7—C8—H8A	119.0	N1—C15—H15C	109.5
C8—C9—C10	127.7 (2)	H15A—C15—H15C	109.5
C8—C9—H9A	116.2	H15B—C15—H15C	109.5
C10—C9—H9A	116.2		
C6—C1—C2—C3	-0.1 (4)	C1—C6—C7—C8	-176.6 (2)
C1—C2—C3—O2	-179.5 (2)	O1—C7—C8—C9	-5.6 (4)
C1—C2—C3—C4	0.5 (4)	C6—C7—C8—C9	172.7 (2)
O2—C3—C4—C5	179.4 (2)	C7—C8—C9—C10	-179.5 (2)
C2—C3—C4—C5	-0.6 (4)	C8—C9—C10—C11	-8.4 (4)
C3—C4—C5—C6	0.3 (4)	C8—C9—C10—C12	172.3 (2)
C4—C5—C6—C1	0.0 (4)	C12—C10—C11—C12 ⁱ	-0.5 (4)
C4—C5—C6—C7	-179.3 (2)	C9—C10—C11—C12 ⁱ	-179.8 (2)
C2—C1—C6—C5	-0.1 (4)	C11—C10—C12—C11 ⁱ	0.5 (4)
C2—C1—C6—C7	179.3 (2)	C9—C10—C12—C11 ⁱ	179.8 (2)
C5—C6—C7—O1	-179.0 (2)	C14—N1—C13—O3	-179.1 (3)
C1—C6—C7—O1	1.7 (4)	C15—N1—C13—O3	-0.8 (4)
C5—C6—C7—C8	2.7 (4)		

Symmetry code: (i) $-x+1, -y+2, -z$.

Hydrogen-bond geometry (\AA , $^\circ$)

$D-H\cdots A$	$D-H$	$H\cdots A$	$D\cdots A$	$D-H\cdots A$
O2—H2B \cdots O3 ⁱⁱ	0.99 (4)	1.63 (5)	2.592 (3)	162 (4)

Symmetry code: (ii) $-x, -y, -z+1$.